Int. J. Heat Mass Transfer. Vol. 10, pp. 1861–1873. Pergamon Press Ltd. 1967. Printed in Great Britain

LAMINAR FLOW HEAT TRANSFER FROM AN ARGON PLASMA IN A CIRCULAR TUBE

F. P. INCROPERA† and G. LEPPERT

Department of Mechanical Engineering, Stanford University, Stanford, California

(*Received* 14 *December* 1966 *and in revised form* 3 *July* 1967)

Abstract—The laminar flow of a plasma in the entrance region of a circular tube has been analyzed using an implicit finite-difference scheme. The solution is based upon the boundary-layer equations with the plasma radiation term retained in the energy equation, and the transverse convection term retained in both the momentum and energy equations. Numerical results have been obtained for an argon plasma having a linear enthalpy and cubic velocity profile at the tube entrance. At the low temperature limit of the analysis, the friction factor is in agreement with previously published results; and in all but a very small region near the tube entrance the local Nusselt number agrees with the Nusselt number for constant property, fully-developed flow to within approximately 17 per cent.

NOMENCLATURE

c_p, specific heat;
c_p^+, non-dimensional specific heat, $c_p/c_{p,0}$;
f, friction factor;
g, acceleration of gravity;
g', conductance based on enthalpy difference;
G, mass velocity, $\rho_0 u_0$;
h, enthalpy;
h^+, non-dimensional enthalpy, $(h/c_{p,0}T_0)$;
h', Planck constant;
j, particular ionization level;
k, thermal conductivity;
k^+, non-dimensional thermal conductivity, k/k_0;
k', Boltzmann constant;
M_0, Mach number, $u_0/(\gamma_0 R T_0)^{\frac{1}{2}}$;
n, particle number density;
N_{Gr}^*, modified Grashof number, $8g\rho^2 r_0^3/\mu^2$;
N_{Nu}, Nusselt number, $2q_w'' r_0[k(T_w - T_m)]$;
N_{Pr}, Prandtl number, $c_p\mu/k$;
N_{Re}, Reynolds number, $2(\rho u)_m r_0/\mu$;
p, static pressure;
p^+, non-dimensional pressure, p/p_0;
P, pressure defect, $(p_0 - p)/(\rho_0 u_0^2)$;
P_R, continuum plasma radiation;
P_R^+, non-dimensional plasma radiation, $2r_0^2 P_R/k_0 T_0$;
q_w, heat flux at tube wall;
q^+, non-dimensional heat flux, $r_0 q_w''/k_0 T_0$;
r, radial coordinate;
r_0, tube radius;
r^+, non-dimensional radius, r/r_0;
R, gas constant;
T, temperature;
T_0, reference temperature corresponding to bulk enthalpy at tube inlet;
u, axial velocity component;
u_0, mean velocity at tube inlet;
u^+, non-dimensional radial velocity, u/u_0;
v, radial velocity component;
v^+, non-dimensional radial velocity, $(v/u_0)N_{Re,0}N_{Pr,0}$;
x, axial coordinate;
x^+, non-dimensional axial coordinate, $x/(r_0 N_{Re,0} N_{Pr,0})$;
Z, effective ionic charge.

Greek symbols

α, degree of ionization;
γ, ratio of specific heats;
ε_ν, emission coefficient;
θ, non-dimensional temperature, T/T_0;
ν, spectral frequency;

† Present address: Department of Mechanical Engineering, Purdue University, Lafayette, Indiana.

ν_g, cutoff frequency;
μ, viscosity;
μ^+, non-dimensional viscosity, μ/μ_0;
ρ, density;
ρ^+, non-dimensional density, ρ/ρ_0;
τ_w, wall shear stress, $[-\mu(\partial u/\partial r)]_{r=r_0}$;
τ_w^+, non-dimensional wall shear stress, $[-\mu^+(\partial u^+/\partial r^+)]_{r^+=1}$.

Subscripts

CL, centerline conditions;
e, refers to an electron;
j, refers to a particular ionization level;
m, mixed mean value with respect to tube cross-section;
0, gas properties evaluated at the bulk tube inlet conditions;
w, tube wall condition.

INTRODUCTION

WITH the advent of extremely high temperature nuclear reactors, hypervelocity flight, and magnetogasdynamic energy conversion techniques, there has been considerable effort devoted to the study of the plasma state. One of the most commonly used plasma sources is the electric arc, and tube arcs are presently being considered for use as space propulsion devices, in hypersonic wind tunnels, and in MHD accelerators. In addition tube arcs and the resulting high temperature plasma are being used for chemical synthesis and in the study of high temperature transport properties.

In recent years there has been a rapid growth in the amount of research devoted to the analysis of the internal flow of high temperature gases. The use of constant property solutions may lead to significant errors in the treatment of flows with gas properties which vary considerably over the tube cross-section, and for this reason the present trend is towards the use of numerical techniques.

Deissler [1] was among the first to report a solution for the laminar flow of a gas with non-constant properties, and improvements in the analytical approach were later made by Sze [2] and Davenport and Leppert [3]. In most cases the agreement of predicted Nusselt numbers and friction factors with available experimental results was poor.

Following a suggestion by Davenport [3], Worsøe-Schmidt and Leppert [4] used an implicit finite-difference scheme to solve the complete boundary-layer equations which included radial convection. Numerical results were obtained for air with both uniform wall heat flux and uniform wall temperature and for wall-to-bulk temperature ratios which varied from 0·5 to 4 (temperature range from 300 to 1700°K).

While other investigators [2–4] have treated the problem of the perturbation of a developed velocity profile by moderate variation of gas properties, the present study is concerned with the influence on the flow field of gas properties which may vary by several orders of magnitude over the tube cross-section. The laminar flow of a plasma in the entrance region of a cooled circular tube is solved using a finite-difference technique similar to that employed by Worsøe-Schmidt and Leppert. Numerical results are obtained for argon with a constant wall temperature boundary condition and for wall-to-bulk temperature ratios which vary from approximately 0·05 to 0·4.

GOVERNING EQUATIONS

Consider an externally cooled, constant wall temperature circular tube mounted vertically on (but electrically insulated from) a tube arc. Convective and radiative cooling take place downstream of the tube entrance, and initial velocity and enthalpy profiles are employed which are representative of conditions measured at the exit plane of the tube arc [5].

The complete set of coupled differential equations which govern the plasma flow are elliptic and highly nonlinear. The solution of such a set of equations would require use of an iterative relaxation scheme with large convergence times. To make the problem more

amenable to solution, a number of assumptions have been employed.

The flow is assumed axisymmetric and steady. Arc instabilities, which could strongly influence the flow variables, are assumed to exist only in regions upstream of the tube entrance.

Molecular contributions to the axial transfer of momentum and energy are neglected. For laminar, constant property flow, thermal conduction in the axial direction is known to be negligible for values of $N_{Re}\,N_{Pr}$ greater than about 100 [6]. Since high temperatures increase convective as well as molecular energy transport processes, there is no reason to believe that this criterion will not be applicable. In the present problem the value of $N_{Re}N_{Pr}$ is at worst slightly lower than 100, and the assumption of negligible axial thermal conduction is therefore a valid one. Since the Prandtl number is approximately unity over the entire temperature range, it is also reasonable to neglect molecular contributions to axial momentum transfer. In addition the remaining boundary-layer approximations are assumed valid.

Only three species are assumed to be present in the plasma, neutral and singly-ionized argon atoms and free electrons. This assumption is valid in argon up to 19000°K, above which the concentration of doubly-ionized atoms becomes appreciable. Each of the species is assumed to obey the perfect gas thermal equation of state. In addition the plasma is assumed to be in a state of local thermodynamic equilibrium. As discussed by Bahadori and Soo [7] and Jacobs and Grey [8], this assumption may be expected to hold in all but a small region near the tube wall. The diffusion of ions and electrons which takes place is assumed to be ambipolar, and diffusion-thermo and thermo-diffusion effects are neglected. The gas is assumed to be optically thin, and the interior walls of the tube are assumed to be thermally black.

The boundary-layer equations are then

$$\frac{\partial}{\partial x}(\rho u) + \frac{1}{r}\frac{\partial}{\partial r}(r\rho v) = 0 \tag{1}$$

$$\rho\left(u\frac{\partial u}{\partial x} + v\frac{\partial u}{\partial r}\right) = -\rho g - \frac{\mathrm{d}p}{\mathrm{d}x} + \frac{1}{r}\frac{\partial}{\partial r}\left(r\mu\frac{\partial u}{\partial r}\right) \tag{2}$$

$$\rho\left(u\frac{\partial h}{\partial x} + v\frac{\partial h}{\partial r}\right) = u\frac{\mathrm{d}p}{\mathrm{d}x} + \frac{1}{r}\frac{\partial}{\partial r}\left(r\frac{k}{c_p}\frac{\partial h}{\partial r}\right) + \mu\left(\frac{\partial u}{\partial r}\right)^2 - P_R. \tag{3}$$

It should be noted that three terms which are often neglected have been retained. The plasma radiation can be appreciable at these temperatures and, as such, it may have a significant effect on the character of the developing temperature profiles. The radial convection term appearing in the momentum equation is retained because of the strong influence the non-constant property effect is expected to have on the velocity profile development. Although the mechanical dissipation effect is expected to be small for the present application, the $\mu(\partial u/\partial r)^2$ portion of the viscous dissipation term is retained in anticipation of future applications where the effect may be appreciable. The thermal equation of state is

$$\frac{p}{\rho} = (1 + \alpha)RT \tag{4}$$

and the caloric equation of state is given by

$$h = \int_0^T c_p\,\mathrm{d}T. \tag{5}$$

The variation with temperature of the thermodynamic and transport properties for an atmospheric argon plasma is taken from the results of Drellishak, Knopp and Cambel [9] and de Voto [10], respectively.

The boundary conditions are as follows

$$\left.\begin{aligned} u(x, r_0) = v(x, r_0) = 0 \\ \left(\frac{\partial u}{\partial r}\right)_{r=0} = v(x, o) = 0 \end{aligned}\right\} \tag{6}$$

and

$$\left.\begin{aligned} h(x, r_0) = h_w \\ \left(\frac{\partial h}{\partial r}\right)_{r=0} = 0. \end{aligned}\right\} \tag{7}$$

Equations (6) arise from the wall impermeability and zero-slip conditions as well as from the assumption of rotational symmetry. Equations (7) result from the constant wall temperature boundary condition and the assumption of rotational symmetry.

Some care must be exercised in specifying the initial conditions to be used in the analysis. Since the present interest is in internal flows produced by a conventional plasma generator, the enthalpy and velocity profiles measured at the exit plane of a plasma generator [5, 11] are used to suggest the form of the tube inlet conditions. The existence of an inflection point in all of the experimentally determined velocity profiles implies that a cubic, rather than a parabolic, profile may best represent the actual inlet conditions. A profile which satisfies the wall and centerline conditions and provides the desired inflection point is given by

$$u(0,r) = \frac{10}{3}u_0\left[1 - 3\left(\frac{r}{r_0}\right)^2 + 2\left(\frac{r}{r_0}\right)^3\right]. \quad (8)$$

The experimentally determined enthalpy profiles are adquately fitted by a straight line passing from the centerline enthalpy to the prescribed wall enthalpy:

$$h(0,r) = 2h_0\left[1 - \left(\frac{r}{r_0}\right)\right] + h_w. \quad (9)$$

Substituting non-dimensional variables into the foregoing equations, one obtains:

$$\frac{\partial}{\partial x^+}(\rho^+u^+) + \frac{1}{r^+}\frac{\partial}{\partial r^+}(r^+\rho^+v^+) = 0 \quad (10)$$

$$\rho^+\left(u^+\frac{\partial u^+}{\partial x^+} + v^+\frac{\partial u^+}{\partial r^+}\right) = -\frac{1}{2}\frac{N^*_{Gr,0}\,N_{Pr,0}}{N_{Re,0}}\rho^+ + \frac{dP}{dx^+} + 2N_{Pr,0}\frac{1}{r^+}\frac{\partial}{\partial r^+}\left(r^+\mu^+\frac{\partial u^+}{\partial r^+}\right) \quad (11)$$

$$\rho^+\left(u^+\frac{\partial h^+}{\partial x^+} + v^+\frac{\partial h^+}{\partial r^+}\right) = M_0^2(\gamma_0 - 1) \times \left\{2N_{Pr,0}\,\mu^+\left(\frac{\partial u^+}{\partial r^+}\right)^2 - u^+\frac{dP}{dx^+}\right\} + \frac{2}{r^+}\frac{\partial}{\partial r^+}\left(r^+\frac{k^+}{c_p^+}\frac{\partial h^+}{\partial r^+}\right) - P_R^+ \quad (12)$$

$$\rho^+ = \frac{p^+}{\theta(1+\alpha)^+} \quad (13)$$

$$h^+ = \int_0^{\theta} c_p^+\,d\theta. \quad (14)$$

The boundary conditions are

$$\left.\begin{aligned} u^+(x^+,1) &= v^+(x^+,1) = 0\\ \left.\frac{\partial u^+}{\partial r^+}\right)_{r^+=0} &= v^+(x^+,0) = 0\\ h^+(x^+,1) &= h^+(\theta_w)\\ \left.\frac{\partial h^+}{\partial r^+}\right)_{r^+=0} &= 0 \end{aligned}\right\} \quad (15)$$

and the initial conditions are

$$u^+(0,r^+) = \tfrac{10}{3}[1 - 3r^{+2} + 2r^{+3}]$$
$$h^+(0,r^+) = 2h_0^+(1 - r^+) + h_w^+. \quad (16)$$

The heat transfer and wall friction are expressed in terms of the parameters used in the study of the internal flow of conventional fluids. A Nusselt number is defined in terms of the difference between the wall temperature, θ_w, and the mixed mean temperature of the gas, θ_m. The mixed mean enthalpy corresponding to the mixed mean temperature is given by

$$h_m^+ = 2\int_0^1 \rho^+u^+h^+r^+dr^+. \quad (17)$$

The Nusselt number is defined as

$$N_{Nu,m} = \frac{2q^+}{k_m^+(\theta_w - \theta_m)} \quad (18)$$

where the normalized wall heat flux is given by

$$q^+ = \left(\frac{k^+}{c_p^+}\frac{\partial h^+}{\partial r^+}\right)_{r^+=1} \quad (19)$$

The friction factor is defined as

$$f = \frac{\tau_w}{\frac{1}{2}(\rho u)_m u_m} \quad (20)$$

which in non-dimensional form becomes

$$fN_{Re,m} = -\frac{2\rho_m^+}{\mu_m^+}\frac{\left(\mu^+\frac{\partial u^+}{\partial r^+}\right)_{r^+=1}}{\int_0^1 \rho^+ u^+ r^+ \,\mathrm{d}r^+}. \quad (21)$$

PLASMA RADIATION

In solving for the flow of a plasma, it is important that radiation from the gas to the tube wall be accounted for. The radiation emitted by an ionized, monatomic gas results from transitions involving both bound and free electrons. The radiation emitted by an electron undergoing a free-free transition was first analyzed by Kramers [12], and the emission coefficient is given by

$$\varepsilon_\nu = 6{\cdot}8 \times 10^{-45} Z^2 \frac{n_e n_j}{T^{\frac{1}{2}}} \exp\left(-\left[\frac{h'\nu}{k'T}\right]\right) \quad (22)$$

where ε_ν is in units of (W-s/cm^3) and the effective ionic charge, Z, is

$$Z = \frac{\sum_j j^2 n_j}{n_e}. \quad (23)$$

The spectral emission coefficient due to combined free-free and free-bound transitions is given by Unsöld [13] as

$$\varepsilon_\nu = 6{\cdot}8 \times 10^{-45} Z^2 \frac{n_e n_j}{T^{\frac{1}{2}}}, \quad (24)$$

and the theory implies that the emission coefficient is frequency-independent up to a certain cutoff frequency, ν_g. Equations (23) and (24) are both obtained from classical considerations, and quantum effects can be accounted for in the form of a multiplicative factor referred to as the Gaunt factor.

The so-called Kramers–Unsöld model may then be used to determine the total continuum radiation. The model assumes that the Unsöld approximation describes the total continuum up to ν_g and that the Kramers theory correctly predicts the radiation intensity for frequencies greater than ν_g. To maintain consistent behavior at the cutoff frequency, the Kramers emission coefficient is forced to match that given by equation (24) at ν_g. This is done by adjusting the constant in the Kramers approximation.

The approach adopted in this study was to fit the Kramers–Unsöld model to available experimental data by adjusting the cutoff frequency. Using a thermistor bolometer with nearly uniform transmissibility over the frequency range $0{\cdot}175 \times 10^{14}$ s^{-1} to $11{\cdot}2 \times 10^{14}$ s^{-1}, Berry and Tankin [14] measured the total radiation from an argon plasma. To compare their data with the Kramers–Unsöld model, therefore, requires integration of equation (22) and (24) over the appropriate portions of the frequency spectrum. Neglecting quantum effects, the total radiated power (W/cm^3) is given by

$$P_R(T) = 6{\cdot}8 \times 10^{-45} Z^2 \left(\frac{n_e n_j}{T^{\frac{1}{2}}}\right)\int_{\nu_1}^{\nu_g} \mathrm{d}\nu + 6{\cdot}8 \times 10^{-45} Z^2 \left(\frac{n_e n_j}{T^{\frac{1}{2}}}\right) \int_{\nu_g}^{\nu_2} \exp\left\{-\left[\frac{h'}{k'T}(\nu - \nu_g)\right]\right\} \mathrm{d}\nu. \quad (25)$$

Using values of ν_1 and ν_2 equal to $0{\cdot}175 \times 10^{14}$ s^{-1} and $11{\cdot}2 \times 10^{14}$ s^{-1} respectively, the radiative power was computed as a function of temperature with ν_g as a parameter. These results were then plotted against the experimental results due to Berry and Tankin, thereby enabling determination of the dependency of cutoff frequency with temperature. With ν_g now known as a function of temperature, values of ν_1 and ν_2 equal to 0 and ∞ respectively may be substituted into equation (25) and the total radiative power determined as a function of temperature. The results of this calculation are shown as the lower curve in Fig. 1.

At the time the calculations were performed, there was some doubt concerning the validity of the Berry and Tankin results. A comparison

of their results with those obtained by Emmons [15] revealed discrepancies of more than an order of magnitude. The source of the discrepancy had not yet been resolved, and the flow calculations were predicated on the Berry

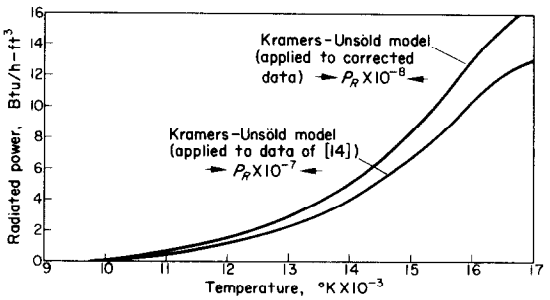

FIG. 1. Radiation from an argon plasma.

and Tankin data. It was recently brought to the authors' attention (reviewer's comments) that an omission of the 4π sr per solid angle resulted in the Berry and Tankin data being too low by a factor of 4π. Inclusion of this factor results in good agreement between their results and those obtained by Emmons.

The numerical calculations were repeated using a plasma radiation model based upon the corrected Berry and Tankin data shown as the upper curve in Fig. 1. The revised calculations are considered to be more representative of the actual flow conditions. Comparison of the two sets of results provides an indication of the extent to which plasma radiation affects the flow development.

NUMERICAL SOLUTION

Reduction of the equations governing the laminar flow of a plasma in a circular tube to parabolic form has been effected by the neglect of the axial transport of momentum and energy due to molecular conduction. Even with the resulting simplifications, however, inherent nonlinearities prevent an analytical treatment of the problem. These nonlinearities appear both explicitly in the momentum equation and implicitly through the dependence on temperature of the gas properties. If oversimplifications in the analytical model are to be avoided and due consideration is to be given to the significant variation in gas properties, finite-difference methods must be employed.

An implicit finite-difference scheme, similar to that used by Worsøe-Schmidt and Leppert [4], was used in a step-by-step solution of the initial value problem. The method employs a central difference representation for the dependent variables in the radial direction and a two-level scheme in the axial or marching direction.

A value of the weighting parameter equal to 0·75 was used in the Taylor series representations of the difference quotients. Such a value was employed by Worsøe-Schmidt and Leppert, and it appears to be a reasonable compromise between conflicting convergence and stability requirements.

The difference quotients are then substituted into the continuity, momentum and energy differential equations, and the resulting difference equations are linearized and uncoupled locally. The continuity equation is uncoupled from the momentum and energy equations, and its solution is deferred until after the axial velocities and enthalpies have been determined. Linearization of the momentum and energy equations is effected through introduction of the values of μ^+, k^+/c_p^+, and ρ^+u^+ from the preceding axial location. Despite the strong coupling between the energy and momentum equations, they are solved independently and iteratively. At all axial stations, except those where the radial step-width is increased, one iteration is used. At each new axial location computations start with known values from the preceding step used as the linearizing terms. In the first iteration, however, weighted average values are used in the linearized terms. A more detailed description of the finite-difference scheme, along with the uncoupling and linearization procedure, is provided by Incropera [11].

Two techniques are used to determine if the convergence of the finite-difference schemes is satisfactory. One technique relies upon a com-

parison of solutions obtained with different mesh sizes, and the second method depends upon application of the momentum theorem and conservation of mass and energy to a control volume analysis. Since the second technique provides a comparison of two numerically determined quantities for each of the three conservation equations, it does not provide an exact measure of the actual error. The convergence check based upon the control volume analysis is therefore regarded as only a partial check on the convergence of the numerical solution, the final check coming with comparison of the numerical results obtained for various values of the axial and radial step-widths.

The problem was coded in FORTRAN IV and solved on the IBM 7090 computer of the Stanford Computation Center. Values of bulk enthalpy and mean velocity at the tube entrance of 4500 Btu/lb and 450 ft/s respectively were chosen. These values provide profiles typical in magnitude to those determined experimentally at the exit plane of a conventional plasma generator [5]. The equilibrium temperature corresponding to the prescribed enthalpy is 21035°R, and the tube diameter is taken to be 0·4 in. The corresponding value of $N_{Re,0}$ is 218, for which the plasma flow is laminar [16]. The tube wall is considered to be at a uniform temperature of 1000°R. The analysis is carried out to a value of $x^+ = 0{\cdot}4$, which corresponds to a tube length-to-diameter ratio of approximately sixty.

Although the mesh size plays a significant role in determining the convergence of the finite-difference scheme, the manner in which the step sizes are optimized is arbitrary. To check the convergence characteristics, computer runs were made for three mesh sizes. The first run was made with an axial step-width of $2{\cdot}5 \times 10^{-5}$ and a radial step-width of $1{\cdot}25 \times 10^{-2}$ at the tube entrance. Successive runs were made with an axial step-width of $2{\cdot}0 \times 10^{-5}$ and radial step sizes of $8{\cdot}33 \times 10^{-3}$ and $6{\cdot}25 \times 10^{-3}$. Since a finer mesh is needed at the tube entrance, where property variations are extreme, the program was written such that the axial and radial step-widths could be increased as the solution progressed. The computation times varied from a minimum of 25 min to a maximum of 50 min for the three grid sizes considered.

From the numerical results obtained for successively smaller step-widths and the convergence checks obtained from the control volume analyses, it was found that for the most part the finite-difference scheme did converge. The velocity and temperature profiles computed at a prescribed axial station for the three mesh sizes agree to within 3 per cent, and the secondary checks on the mass and momentum flux are satisfied to within a few per cent. The check on the local energy flux, however, indicated that conservation of energy was not satisfied near the tube entrance.

For the largest of the three grid sizes employed, the relative error in the mean enthalpy flux attained a maximum value of 87 per cent at $x^+ = 0{\cdot}03$ and decreased steadily through the remainder of the tube. For the intermediate and smallest mesh sizes, the relative error in the enthalpy flux attained maximum values of 64 per cent and 50 per cent, respectively. These results indicate that as much as a 40 per cent reduction in the error in the mean enthalpy flux results in at most a three per cent change in the velocity or temperature at a given location.

Although the profiles and friction factors compared favorably from one mesh size to the next, the values of the wall heat transfer and local Nusselt number in the entrance region of the tube did not. In general it was found that these quantities increased significantly with each decrease in step-width. This behavior suggested that failure of the energy balance check to indicate convergence was due to errors in computation of the wall heat flux.

The approach taken in this study was to express temperature as a power series expansion from the wall and to evaluate the local heat flux by taking the slope. A cubic polynominal was used with coefficients determined from function

values at three interior points. Such an approach is customarily adequate for computing wall heat transfer, but with the extremely large temperature gradients encountered near the wall in the tube flow (see Fig. 4), it may lead to considerable error.

To further examine this condition, the wall heat flux was computed a second way. From an energy balance performed on a control volume set up about an arbitrary axial location, the heat transfer at the wall may be expressed as

$$q^+ = -\frac{1}{2}\left[\frac{\mathrm{d}}{\mathrm{d}x^+}\left(\int_0^1 \rho^+ u^+ h^+ r^+ \,\mathrm{d}r^+\right) - \int_0^1 P_R^+ r^+ \,\mathrm{d}r^+\right]. \quad (26)$$

Using this equation, the dimensionless convective heat flux was computed at several locations along the tube axis. Since the mixed mean enthalpy is known to better than 1 per cent accuracy, the resulting values of q^+ are known to the accuracy with which the required slopes may be found. A comparison of the heat flux computed from the wall slope and energy balance techniques is shown in Table 1.

Table 1. Comparison of wall heat flux computed from wall slope (q_1^+) and energy balance (q_2^+) techniques

x^+	q_1^+	q_2^+
0·00008	−0·292	−1·066
0·016	−0·354	−0·563
0·04	−0·286	−0·419
0·12	−0·120	−0·122
0·16	−0·067	−0·069
0·24	−0·027	−0·028
0·32	−0·014	−0·015

Immediately obvious is the large discrepancy appearing between the two values of heat flux computed at stations near the tube entrance. At locations further downstream the differences become smaller, and beyond $x^+ = 0{\cdot}12$ they are within the accuracy with which q_2^+ is determined. Such a comparison verifies the premise that the errors encountered in the energy balance conversion check are the result of errors in the computation of wall heat flux.

On the basis of the foregoing results it may be concluded that the velocity and temperature profiles and the local friction factor are known to within an accuracy of a few per cent over the entire length of the tube flow. The wall slope technique of computing convective heat transfer at the tube boundaries results in considerable underprediction of the local heat flux and Nusselt number in regions near the tube entrance. Improvement of this latter condition may be effected through use of an energy balance technique for computation of the wall heat flux.

RESULTS

For the prescribed inlet conditions Figs. 2–4 show the development of the axial and radial velocity profiles and the temperature profile. The results were obtained using the corrected Berry and Tankin data to account for plasma radiation effects (upper curve of Fig. 1). Several important qualitative effects are immediately obvious from Fig. 2. As energy passes from the

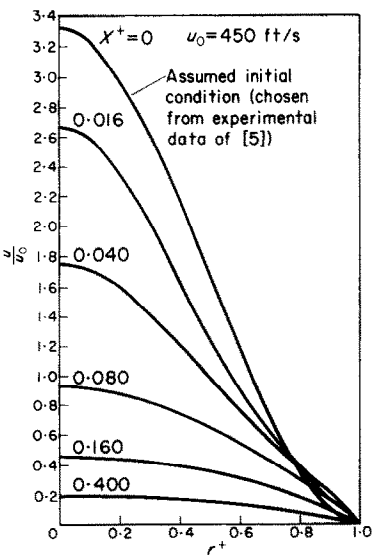

FIG. 2. Axial velocity profiles.

plasma to the tube wall, the gas temperature must drop, giving rise to an increase in density. Conservation of mass requires that the flow must then decelerate. The considerable reduction in velocity which occurs as the gas passes from the tube entrance to $x^+ = 0{\cdot}4$ reflects the order-of-magnitude change in density

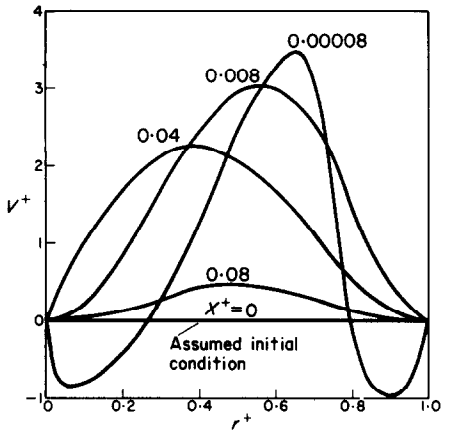

FIG. 3. Radial velocity profiles.

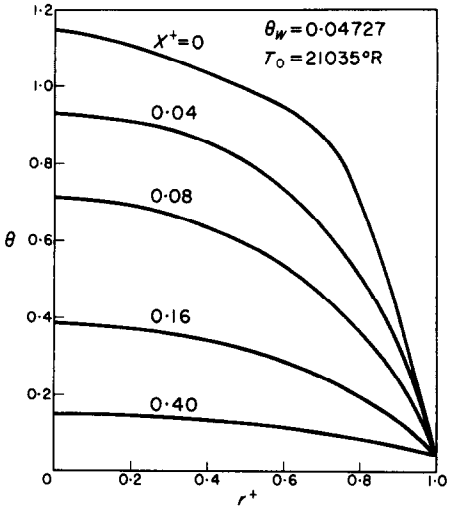

FIG. 4. Temperature profiles.
Assumed initial conditions (chosen from experimental data of [5]).

which must occur as the gas proceeds from a highly ionized condition to a relatively cool state. Of interest also is the fact that the initially cubic profile takes on a nearly parabolic shape as the gas cools, thereby demonstrating a tendency for the hydrodynamic flow to approach a fully-developed, constant-property condition. This behavior is verified by the radial velocity profiles presented in Fig. 3. Although the transverse velocity component is significant in regions near the tube entrance, it becomes negligible beyond $x^+ = 0{\cdot}08$, the station at which the axial velocity profile begins to assume a parabolic shape.

The axial velocity may also be normalized with respect to the local mean velocity rather than the reference velocity used in Fig. 2. In so doing the resulting profiles are changed by very little in the range from $x^+ = 0{\cdot}08$ to $x^+ = 0{\cdot}4$, again indicating the existence of a virtually fully-developed, hydrodynamic flow in that range.

Figure 4 shows the temperature profiles which exist at various locations along the tube axis. The temperature is normalized with respect to the reference condition to indicate clearly the amount of cooling which occurs. The temperature profiles were also plotted in the more conventional manner, that is, $T_w - T/T_w - T_m$ as a function of r^+; there is nothing to indicate

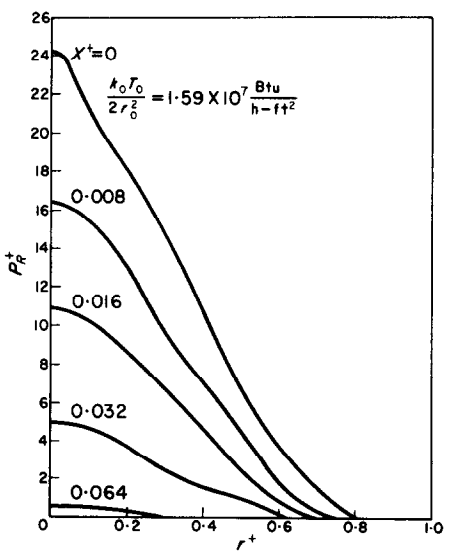

FIG. 5. Profiles of plasma power radiated per unit volume.

that these profiles become fully-developed before $x^+ = 0{\cdot}40$.

Figure 5 provides profiles of the power radiated per unit volume at several stations along the tube axis. It should be noted that plasma radiation is only significant in the first 20 per cent of the tube length considered. Beyond $x^+ = 0{\cdot}08$ the effect of radiation on flow field development is negligible.

The flow profiles were also computed with the radiation accounted for using the original Berry and Tankin data [14], as well as for the case of zero radiation. The effect of increasing the magnitude of the plasma radiation term is one of enhancing the deceleration and cooling processes. Although the magnitude of the velocity components and the temperature at a particular location in the tube may vary appreciably with the radiation model, the general shape of the profiles is preserved. For the three cases considered, the hydrodynamic flow is to a good approximation fully-developed at $x^+ = 0{\cdot}08$.

Figure 6 shows the axial distribution of the

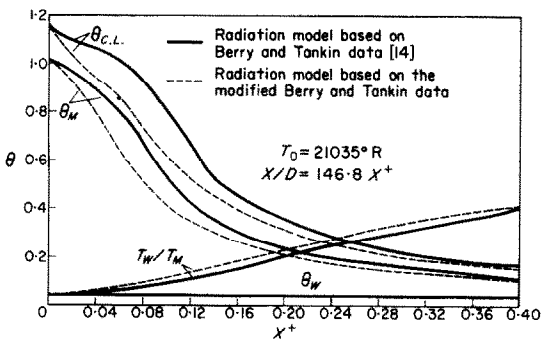

FIG. 6. Axial distribution of centerline, mixed mean, and wall temperature.

centerline temperature, θ_{CL}, the equilibrium temperature, θ_m, corresponding to the mixed mean enthalpy, h_m, and the wall to bulk temperature ratio, T_w/T_m. To gain some appreciation for the effect of radiation on flow field development, the computations were carried out with the radiation model based upon both the original and the corrected Berry and Tankin data. As expected, use of the corrected radiation model results in an appreciable reduction in θ_{CL} and θ_m in the intermediate areas of the tube. For both radiation models, however, the centerline and mixed-mean temperatures pass from 24200°R and 21400°R, respectively, to final values of approximately 3400°R and 2500°R in approximately sixty tube diameters. Analogous trends appear for the wall to bulk temperature ratio.

In Fig. 7 the friction factors computed in the

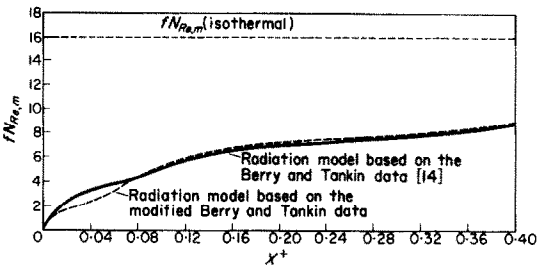

FIG. 7. Local friction factor for plasma flow in a circular tube.

present study are compared with the known value for isothermal flow. That the product of friction factor and Reynolds number is less than the value for isothermal flow and approaches this condition with increasing axial distance is to be expected. Worsøe-Schmidt and Leppert [4] demonstrated that for the cooling of air the value of $fN_{Re,m}$ is less than sixteen at the tube entrance and approaches sixteen as the flow approaches an isothermal condition. In the present study the analysis was extended to an axial location where the wall to mean temperature ratio reached a value of 0·426. The corresponding value of $fN_{Re,m}$ is 8·94. Worsøe-Schmidt and Leppert considered a single gas cooling case where the wall to mean temperature ratio was initially 0·508 and the corresponding value of $fN_{Re,m}$ was 9·23. The fact that the results of the present study for ionized argon blend nicely with existing results for air is encouraging. The implication is that the present results may be used in conjunction with those of Worsøe-Schmidt and Leppert to provide an estimate of $fN_{Re,m}$ in the range of $0{\cdot}1 \leqslant T_w/T_m$

$\leqslant 1{\cdot}0$ which is valid independent of the kind of gas employed. The results obtained for the two radiation models are virtually identical except in the early stages of the flow development ($0 < x^+ < 0{\cdot}07$). The effect of an increase in radiation on flow deceleration appears to be enough to appreciably alter the slope of the axial velocity component near the wall in the entrance region of the tube.

The local Nusselt number was first computed using equation (18) and a radiation model based on the Berry and Tankin data [14]. The results are shown plotted in Fig. 8 and tabulated

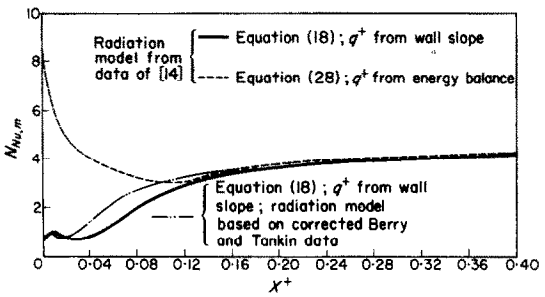

FIG. 8. Local Nusselt number for plasma flow in a circular tube.

Table 2. Local Nusselt number for plasma flow in a circular tube (radiation model based on the data of [14])

x^+	$N^a_{Nu,m}$	$N^b_{Nu,m}$	$N^c_{Nu,m}$	$N^d_{Nu,m}$
0·00008	0·575	2·098	2·553	9·317
0·016	0·799	1·271	3·203	5·095
0·040	0·917	1·343	2·722	3·986
0·120	2·977	3·025	2·977	3·025
0·160	3·401	3·500	3·401	3·500
0·240	3·808	3·907	3·808	3·907
0·320	4·097	4·150	4·097	4·150

a: Nusselt number based on $(\theta_w - \theta_m)$ and q^+ computed using wall slope technique.
b: Nusselt number based on $(\theta_w - \theta_m)$ and q^+ computed using energy balance technique.
c: Nusselt number based on $(h^+_w - h^+_m)$ and q^+ computed using wall slope technique.
d: Nusselt number based on $(h^+_w - h^+_m)$ and q^+ computed using energy balance technique.

$$N^{c,d}_{Nu,m} = \frac{(\theta_w - \theta_m)}{(h^+_w - h^+_m)} c^+_{p,m} N^{a,b}_{Nu,m}.$$

for selected axial locations in column a of Table 2. As discussed previously, the errors associated with computing a Nusselt number using a heat flux based on the wall slope technique are considerable in the tube entrance region. For this reason the Nusselt numbers were recomputed at selected axial locations using the heat flux determined from the energy balance method [equation (26)], and the results are presented in column b of Table 2.

In comparing the results presented in columns a and b of Table 2, we see immediately the effect on $N_{Nu,m}$ of the newly determined heat fluxes. In the range $0 \leqslant x^+ \leqslant 0{\cdot}12$, the Nusselt numbers in column b are significantly larger than those in column a; and for x^+ greater than 0·12, the results are in good agreement. For the tube entrance region, the results in column b are more accurate.

In working with the flow of high temperature gases, it is customary to define the surface heat flux on the basis of an enthalpy difference rather than a temperature difference [6].

$$q''_w = g'(h_m - h_w). \tag{27}$$

The local Nusselt number may then be written as

$$N_{Nu,m} = \frac{q''_w}{(h_m - h_w)} \frac{N_{Pr,m} N_{Re,m}}{G}. \tag{28}$$

Values of $N_{Nu,m}$ based on equation (28) have been computed and are presented in columns c and d of Table 2. Of primary interest are the results in column d which were computed using the wall heat flux determined from the energy balance technique. These results are also shown plotted in Fig. 8.

It is of interest to compare the Nusselt number based upon enthalpy difference and heat flux computed using the energy balance technique to the value of N_{Nu} for the flow of a constant property gas with fully-developed velocity and temperature profiles. For a constant wall temperature boundary condition, N_{Nu} assumes a value of 3·66. Therefore in the range $0{\cdot}03 \leqslant x^+ \leqslant 0{\cdot}40$, the value of $N_{Nu,m}$

agrees with the fully-developed, constant property Nusselt number to within 17 per cent on the low side and 13 per cent on the high side.

The implication of the above result is remarkable when considered in light of the number of effects which influence the local convective heat transfer. A designer may assign a value of 3·66 to the Nusselt number defined by equation (28) and predict with a reasonable degree of accuracy the convective heat transfer from a plasma to the walls of a circular tube everywhere but in a very small region near the tube entrance. This suggests that within a very small distance from the tube entrance, a quasi-fully-developed flow condition prevails. Although the velocity and temperature profiles are not fully developed, energy is transferred to the wall as though such a condition did exist.

The results obtained using a radiation model based upon the corrected Berry and Tankin data and equation (18) in conjunction with the wall slope technique are also plotted in Fig. 8. The deviation from previous results exists exclusively in the entrance region where radiation effects are most significant. The effect of using the corrected radiation is to promote the occurrence of the aforementioned quasi-fully-developed flow condition at a location closer to the tube entrance.

CONCLUSIONS

An implicit finite-difference scheme has been used to solve for the profiles and wall parameters characteristic of the laminar flow of an argon plasma in a circular tube. Due to the form of the assumed inlet conditons and the large variable properties effect prevalent in plasma flows, the solutions presented in this paper lack the generality of the solutions for flows with constant fluid properties. Despite these restrictions, however, it is still possible to draw conclusions of a fairly general nature.

The axial and transverse velocity profiles computed in this study indicate a strong tendency for the hydrodynamic flow to assume a fully-developed condition. Such a fully-developed condition was attained within approximately twelve diameters from the tube entrance. At no point in the flow, however, do the temperature profiles approach a fully-developed condition.

The product of the friction factor and the Reynolds number based upon mean properties, $fN_{Re,m}$, was computed and found to agree in the limit with the results of Worsøe-Schmidt and Leppert [4]. The fact that the present results apply for argon and those due to Worsøe-Schmidt and Leppert apply for air implies that the combined results may be used to provide an estimate of $fN_{Re,m}$ in the range $0{\cdot}1 \leqslant T_w/T_m \leqslant 1{\cdot}0$ which is valid independent of the gas employed.

A Nusselt number is computed based upon enthalpy difference and wall heat flux determined from an energy balance technique. The value of this Nusselt number is large near the tube entrance but drops rapidly in the early stages of flow development. At axial locations greater than approximately four tube diameters, the value of this Nusselt number agrees with the Nusselt number for fully-developed, constant property flow to within 17 per cent on the low side and 13 per cent on the high side. This suggests that, within a very small distance from the tube entrance, a quasi-fully-developed flow condition prevails. Although the velocity and temperature profiles may not be fully developed, energy is convected to the wall as though such a condition did exist.

ACKNOWLEDGEMENTS

This paper is based on a dissertation [11] submitted to Stanford University by F. P. Incropera in partial fulfillment of the requirements for the degree of Doctor of Philosophy. The authors are indebted to Dr. P. M. Worsøe-Schmidt of the Technical University of Denmark, who provided many useful suggestions concerning the numerics of the tube flow analysis; to Professor W. M. Kays of Stanford University, who suggested the problem and provided many stimulating discussions throughout the course of its solution; and to Philip S. Schmidt of Stanford University, who assisted in several important ways. The work was supported by the U.S. Atomic Energy Commission under Contract AT(04-3)-247.

REFERENCES

1. R. G. DEISSLER, Analytical investigation of fully developed laminar flow in tubes with heat transfer with fluid properties variable along the radius, NACA TN 2410 (July 1951).
2. B. C. SZE, The effect of temperature dependent fluid properties in circular tubes, Ph.D. Dissertation, Department of Mechanical Engineering. Stanford University (April 1957).
3. M. E. DAVENPORT and G. LEPPERT, The effect of transverse temperature gradients on the heat transfer and friction for laminar flow of gases, ASME Paper 64-HT-10 (1964).
4. P. M. WORSØE-SCHMIDT and G. LEPPERT, Heat transfer and friction for laminar flow of gas in a circular tube at high heating rate, *Int. J. Heat Mass Transfer* **8**, 1281–1301 (1965).
5. F. P. INCROPERA and G. LEPPERT, Investigation of arc jet temperature measurement techniques. *I.S.A. Trans.* **1**, 35–41 (1967).
6. W. M. KAYS, *Convective Heat and Mass Transfer*. McGraw-Hill, New York (1966).
7. M. N. BAHADORI and S. L. SOO, Non-equilibrium transport phenomena of partially ionized argon, *Int. J. Heat Mass Transfer* **9**, 17–34 (1966).
8. P. F. JACOBS and G. GREY, Criterion for electron-heavy particle nonequilibrium in a partly-ionized gas, AIAA Paper 66-192 (March 1966).
9. K. S. DRELLISHAK, C. F. KNOPP and A. B. CAMBEL, Partition functions and thermodynamic properties of argon plasma, AEDC-TDR-63-146 (August 1963).
10. R. S. DE VOTO, Argon plasma transport properties, Department Aeronautical Engineering, Stanford University, Report SU AA217 (1965).
11. F. P. INCROPERA, Temperature measurement and internal flow heat transfer in an argon plasma, Ph.D. Dissertation, Department Mechanical Engineering, Stanford University (August 1966).
12. H. A. KRAMERS, On the theory of X-ray absorption and of the continuum X-ray spectrum, *Phil. Mag.* **46**, 836–871 (1923).
13. A. UNSÖLD, Über das Kontinuierliche Spectrum der Hg-Hochdrucklampe des Unterwasserfunkens und ahnlicher Gosentladungen, *Ann. Phys.* **33**, 607–616 (1923).
14. J. M. BERRY and R. S. TANKIN, An experimental study of radiant energy transfer from a plasma, AEDC-TDR-64-233 (November 1964).
15. H. W. EMMONS, The arc measurement of high temperature gas transport properties, Harvard University Engineering Sciences Laboratory TR No. 23 (1965).
16. F. P. INCROPERA and G. LEPPERT, Flow transition phenomena in a subsonic plasmajet, *AIAA Jl* **6**, 1087–1089 (1966).

Résumé—L'écoulement laminaire d'un plasma dans la région d'entrée d'un tube circulaire a été analysé en employant un schéma implicite de différences finies. La solution est basée sur les équations de la couche limite en retenant le terme de rayonnement du plasma dans l'équation de l'énergie, et le terme de convection transversale à la fois dans l'équation de la quantité de mouvement et dans celle de l'énergie.

On a obtenu des résultats numériques pour un plasma d'argon ayant à l'entrée du tube un profil d'enthalpie linéaire et un profil de vitesse du troisième degré. A la limite de la théorie pour les basses températures, le coefficient de frottement est en accord avec les résultats publiés auparavant, et le nombre de Nusselt local est en accord partout sauf dans une très petite région près de l'entrée du tube avec le nombre de Nusselt pour l'écoulement entièrement établi et à propriétés constantes avec une marge d'environ 17 pour cent.

Zusammenfassung—Die laminare Strömung eines Plasmas im Einlaufbereich eines Rohres von Kreisquerschnitt wurde mit Hilfe eines impliziten endlichen Differenzenschemas analysiert. Die Lösung beruht auf den Grenzschichtgleichungen, wobei der Plasmastrahlungsausdruck in der Energiegleichung und der Querkonvektionsausdruck sowohl in der Bewegungsgleichung als auch in der Energiegleichung enthalten ist. Numerische Ergebnisse wurden an einem Argonplasma für ein lineares Enthalpie- und ein kubisches Geschwindigkeitsprofil am Rohreinlauf erhalten. Innerhalb des kleinen Temperaturbereiches der Analyse stimmt der Reibungskoeffizient mit kürzlich veröffentlichten Ergebnissen überein und ausser einem sehr kleinen Bereich nahe dem Rohreinlauf weicht die örtliche Nusselt-Zahl von der Nusselt-Zahl für konstante Stoffwerte und voll ausgebildete Strömung um nicht mehr als etwa 17% ab.

Аннотация—С помощью неявной конечноразностной схемы анализируется ламинарное течение плазмы во входной области круглой трубы. Решение основано на уравнениях пограничного слоя, где в уравнении энергии сохраняется член излучения плазмы, а в уравнениях момента и энергии — член радиальной конвекции. Получены численные результаты для аргонной плазмы, обладающей линейным профилем энтальпии и кубическим профилем скорости во входной области трубы. При нижнем температурном пределе данного анализа коэффициент трения согласуется с уже опубликованными результатами, а во всей, хотя и очень узкой области около входа в трубу, локальное число Нуссельта согласуется (с точностью около 17%) с числом Нуссельта для полностью развитого течения при постоянных свойствах.